ECCOMAS Congress 2016
VII European Congress on Computational Methods in Applied Sciences and Engineering
M. Papadrakakis, V. Papadopoulos, G. Stefanou, V. Plevris (eds.)
Crete Island, Greece, 5–10 June 2016

MODELING OF PATIENT-SPECIFIC CASES OF ATHEROSCLEROSIS IN CAROTID ARTERIES

Timur Gamilov[1,2], Roman Pryamonosov[1,2] and Sergey Simakov[1,2]

[1]Moscow Institute of Physics and Technology
9, Institutskiy per.,Dolgoprudny, Russia
e-mail: gamilov@crec.mipt ru

[2] Institute of Numerical Mathematics RAS
8, ul. Gubkina, Moscow, Russia

Keywords: Circle of Willis, Patient-specific, Carotid artery stenosis, Vessel segmentation, Microcirculation, 1d haemodynamics

Abstract. *1D model is used to simulate blood flow in major vessels of the upper body and head. The 1D part is stated in terms of viscous incompressible fluid flow in the network of elastic tubes. Two different types of junctions are considered: junctions between major vessels and junctions between arteries and veins. Vessel network reconstruction algorithm consists of vessel segmentation, thinning-based obtaining of set of centerlines, and graph reconstruction. Input data is 3D DICOM datasets, obtained with contrast enhanced Computed Tomography (CT) Angiography. Constructed model is used to study the influence of carotid artery stenosis on the direction of blood flow in the circle of Willis.*

1 Introduction

Investigation of pulsatile blood flow in cerebral normal and diseased vessels provides important information for clinical diagnosis. One-dimensional modelling is a well-developed approach in this area [1, 2]. It allows to simulate large number of arteries and veins and take into account regulatory mechanisms. Computational costs of such approach allow to run numerous numerical experiments in a short time on a laptop. 1D models can be used to study the impact of stenosis on blood flow patterns in cerebral region for different groups of patients. They can also help to choose the most optimal strategy of treatment.

The structure of circle of Willis can be very individual. Simulations based on pre-made averaged vessel structures could produce huge errors. This increases the importance of patient-specific approach in simulations of cerebral blood circulation.

In this work the 1D blood flow model [3] is used to investigate the impact of a stenosis in internal carotid artery on blood flow in the circle of Willis. Microcirculation regions between arteries and veins are simulated with the help of Poiseuille's pressure drop condition. An important feature of this work is reconstruction of patient-specific vessel structure based on CT images.

2 Methods

2.1 Blood flow model

1D haemodynamics model used in this work is the model of viscous incompressible fluid in a network of elastic tubes. Network of arteries is obtained from patient's CT images. Veins are considered to have the same structure as arteries, but different parameters. In this section brief description of the model is presented, for details we refer to [3, 4]. Blood flow in each vessel is described by hyperbolic set of mass and momentum balances

$$\partial A_k/\partial t + \partial(A_k u_k)/\partial x = 0, \tag{1}$$

$$\partial u_k/\partial t + \partial\left(u_k^2/2 + p_k/\rho\right)/\partial x = f_{fr}(A_k, u_k), \tag{2}$$

where k is the index of the vessel; t is the time; x is the distance along the vessel counted from the vessel junction point; ρ is the blood density (constant); $A_k(t,x)$ is the vessel cross-section area; p_k is the blood pressure; $u_k(t,x)$ is the linear velocity averaged over the cross-section; f_{tr} is the friction force. Relationship between pressure and cross-section is given by wall-state equation:

$$p_k(A_k) - p_{*k} = \rho_w c_k^2 f(A_k), \tag{3}$$

where ρ_w is the vessel wall density (constant); $f(A)$ is function

$$f(A_k) = \begin{cases} \exp\left(A_k/A_{0k} - 1\right) - 1, & A_k/A_{0k} > 1 \\ \ln A_k/A_{0k}, & A_k/A_{0k} \leqslant 1, \end{cases} \tag{4}$$

p_{*k} is the pressure in tissues surrounding the vessel; A_{0k} is the unstressed cross-sectional area; c_k defines elastic properties of the wall and can be considered as velocity of small disturbances propagation [5].

At the terminal point of the venous system the pressure $p_H = 8mmHg$ is set as the boundary condition. At the entry point of the aorta the blood flow is assigned

$$u(t,0)\,A(t,0) = Q_H(t). \tag{5}$$

Here function $Q_H(t)$ corresponds to the heart rate value of 1 Hz and stroke volume of 65 ml [6].

Bifurcation points are divided into two groups: 1) common junctions (between arteries and arteries or veins and veins); 2) microcirculation junctions (between arteries and veins). At common junctions continuity of pressure is postulated

$$p_i\left(A_i\left(t,\tilde{x}_i\right)\right) - p_j\left(A_j\left(t,\tilde{x}_j\right)\right) = 0, \tag{6}$$

where i, j are indexes of the vessels. At junction point between M arteries and veins the Poiseuille's pressure drop condition is used

$$p_k\left(A_k\left(t,\tilde{x}_k\right)\right) - p_{node}\left(t\right) = \varepsilon_k R_k A_k\left(t,\tilde{x}_k\right) u_k\left(t,\tilde{x}_k\right), k = k_1, k_2, \ldots, k_M, \tag{7}$$

where R_k represents the hydraulic resistance of *k*-th vessel in the junction; $\varepsilon = 1, \tilde{x}_k = L_k$ for incoming vessels, $\varepsilon = -1, \tilde{x}_k = 0$ for outgoing vessels; p_{node} is the pressure in the junction. Parameters R_k are adjusted to simulate pressure drop between arteries and veins. To close the system, we add the mass conservation condition and compatibility conditions of hyperbolic set (1),(2) (see [4]).

2.2 Reconstruction of patient specific vessel structure

Vessel network reconstruction algorithm consists of vessel segmentation, thinning-based extraction of centerlines, and graph reconstruction [11]. Input data is 3D DICOM datasets, obtained with contrast enhanced Computed Tomography Angiography. Resolution of each 2D transverse slice is 512x512 voxels. Only quasi-isotopic voxel grids with deviation from cubic grids less than 10% were used; other grids can be resampled into isotopic ones.

Anatomy of cerebral vessels in human body is represented by carotid arteries rooting at aorta, vertebral arteries separating from subclavian arteries (that also rooting at aorta), and small arteries in brain. Carotid and vertebral arteries merge in the circle of Willis that allows blood bypass stenoses in neck vessels.

Since all arteries studied originate from aorta, it is natural to segment aorta first (Fig. 2.2 (d)). Our method utilize Hough Circleness [8] and IDT algorithm [9] to produce the aorta mask [11]. Firstly, on the bottommost slice of dataset Hough Circleness algorithm finds largest bright disk corresponding to aorta cut. Secondly, using lowest intensity inside the aorta cut as the threshold we obtain mask M. This mask usually consists of aorta, cerebral vessels, and other bright tissues. Thirdly, IDT algorithm cuts mask M at bottlenecks and outputs mask M_A including aorta and some parts of cerebral and coronary vessels. Finally, morphological operations are used to remove these vessel parts from M_A.

Second segmentation step is to decrease intensities of bones (Fig. 2.2 (c)). We use multi-scale MMBE algorithm [10] which requires two datasets: enhanced with contrast agent and not enhanced. This is the main drawback of our method because every patient has to experience procedure twice and obtains double dose of radiation. However, this step is essential because vertebral arteries are very hard to separate from neck bones on CT images.

Once the bones are darkened, Frangi Vesselness filter [7] is used to segment arteries (Fig. 2.2 (e)). Rather than assuming that the segmentation is the biggest connectivity component of voxels with high vesselness values, we search for all such voxel connectivity components next to the aorta mask. This approach considers that stenoses may divide carotid and vertebral arteries in several parts.

Finally, segmentation errors near the aorta border must be removed (Fig. 2.2 (f)). Despite Frangi Vesselness effectiveness, it can produce segmentation "leaks" near large bright structures

like aorta. Let us denote the mask of cerebral vessels by M_v. Leak removal is represented by iterative procedure working with voxel layers L_i. Each layer L_i is a set of voxels in mask M_v separated from the aorta border by i voxels. On every iteration algorithm removes voxels from layer L_i that have no adjacent voxels in layer L_{i+1}. Algorithm iterating for parameter values $i = i_{max} \dots 1$. Start parameter value i_{max} must be bigger than thickness of "leak" and experiments has shown that i_{max} can be set to 15 voxels.

Entire segmentation algorithm is shown in Fig. 2.2. Bone removal and aorta segmentation are independent steps and may be performed in any order. If the aorta is segmented first, the initial mask M will contain neck bones and skull as shown in Fig. 2.2 (d2).

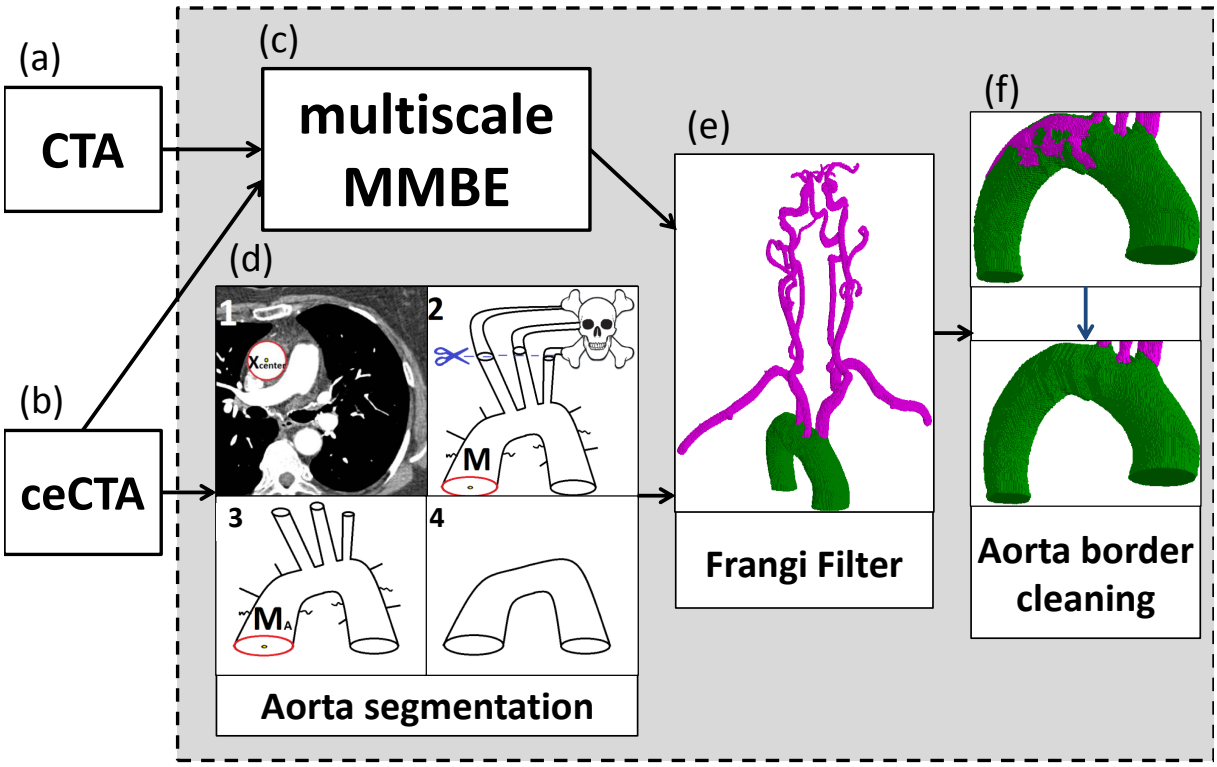

Figure 1: Segmentation algorithm takes (a) CT angiography image and (b) contrast enhanced CT image; (c) bones are removed by multiscale Matched Mask Bone Elimination; (d) essential steps of aorta segmentation: (d1) Hough Circleness, (d2) IDT algorithm cuts mask M at bottlenecks, removing bones and other bright structures and producing (d3) mask M_A, (d4) aorta arch branches and coronary vessels are removed from M_A via morphological operations; (e) cerebral arteries are segmented by Frangi Vesselness Filter; (f) cleaning of aorta border. Mask of aorta is shown by green, cerebral arteries are purple.

After the segmentation, vessel centerlines are extracted with a version of Thinning method with False Twigs Elimination algorithm [11]. These centerlines are used to produce a graph of arterial network where each node corresponds to a bifurcation or an end of vessel and to each edge the length and mean radius of corresponding vessel tube are assigned.

2.3 Computational domain

The extracted network of arteries is presented in Fig. 2. The network of veins is assumed to have similar structure and be connected to the arteries at terminal points. Parameters c_k and R_k were adjusted so that the model reproduces physiological values of blood flows as well as blood velocities measured in control points. The velocities were measured with the Doppler ultrasound method.

The circle of Willis for this particular patient is not closed and consists of vessels 36-35-28-73-85-10-7. The stenosis with degree 90 % is located in the left internal carotid artery. It was simulated by separating the stenosed vessel into three parts: the stenosed part, the proximal part and the distal part. Parameters of the proximal and distal parts correspond to the parameters of the initial non-stenosed vessel. The cross-section of the stenosed part was decreased.

3 Results

Table 1 shows comparison between simulated blood flow velocities and measured velocities for the patient with 90 % stenosis. Measurements after stenosis treatment were not available, so they are substituted by physiological range according to medical literature [6].

Artery (vessel on Fig. 2)	Velocity with stenosis, cm/s						Velocity without stenosis, cm/s	
	Right			Left				
	Sim.	Meas.	Error	Sim.	Meas.	Error	Sim.	Physiol. range
Common carotid (26,3)	50	55	9%	51	54	5.5%	60	50-104
Internal carotid (27,86)	72	67	7%	240	220	10%	48	32-100

Table 1: Simulated blood flow velocities (sim.), measured velocities before stenosis treatment (meas.), physiological range of velocities without stenosis (physiol. range)

Two series of calculation were performed. In the first series all parameters c_k were decreased by 50%, simulating very elastic vessels. In the second series all parameters c_k were increased by 50%, simulating very stiff vessels. Blood flow through vessel 85 (see Fig. 2) was studied for different degrees of stenosis. Results are shown on Fig. 3. Low values of blood flow can be explained by very weak interaction between left and right parts of the Willis circle of the particular patient. Curves in Fig. 3 are almost identical and cross zero line near 54% value.

4 Conclusion

The numerical results show that the proposed vessel network reconstruction algorithm provides a good basis for patient specific simulations. It can be used for the prediction of results of stenosis treatment and for calculation blood flow patterns in hardly accessible regions. The main problems of our approach are necessity to perform two CT scans (with and without contrast) and some difficulties in detection of small vessels in the circle of Willis.

According to Fig. 3, the direction of blood flow in the circle of Willis depends heavily on the degree of stenosis. Certain stenoses can stop blood flow in certain vessels, increasing risk of formation of blood clots. As a result, a relatively weak stenosis (54 %) can be more dangerous than a stronger one.

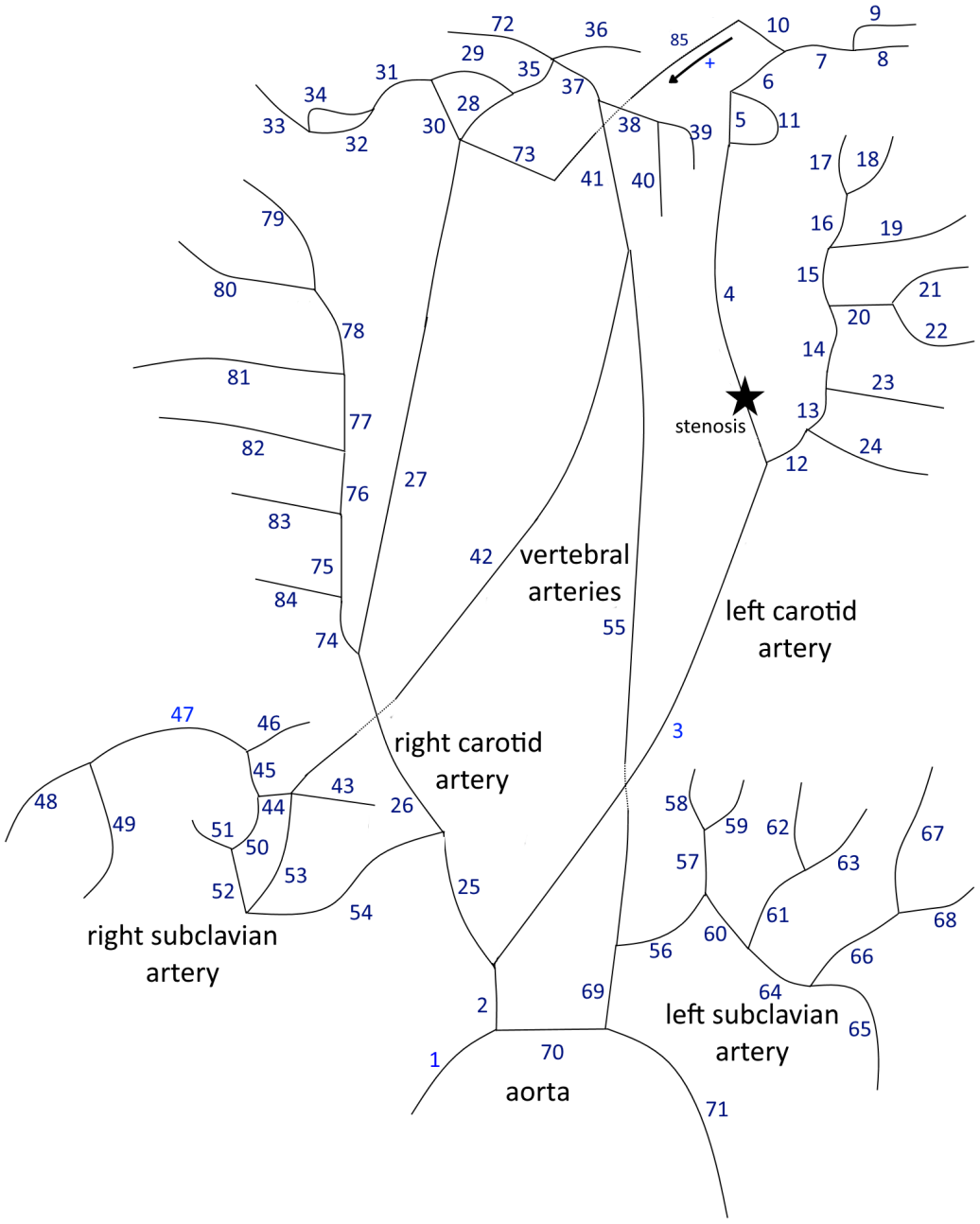

Figure 2: The structure of reconstructed arterial part based on anonymous patient-specific data set. The star designates stenosis. The arrow shows positive blood flow direction in vessel 85. Parameters of the vessels are presented in Tab. 4

Another interesting result is the very small difference between curves for elastic and rigid vessels in Fig. 3. This shows that risks caused by changes in blood flow patterns due to the stenosis are the same for different groups of people: old people, athletes, smokers, etc.

Cerebral blood circulation model presented in this work does not take into account many important regulation mechanisms, such as baroreflex, regulation of CO_2, etc. Regulatory mechanisms are essential in sustaining the blood pressure in cerebral arteries at necessary level. This drawback is partially compensated by pressure continuity condition in bifurcations, but still limits possible applications of the model.

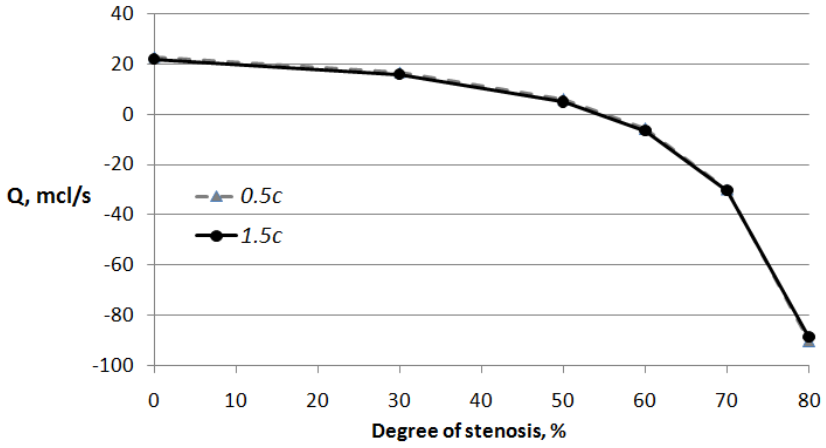

Figure 3: Blood flow in vessel 85 for different degrees of stenosis in left internal carotid artery (see Fig. 2) for elastic vessels ($0.5c$) and rigid vessels ($1.5c$).

Acknowledgement. The research was supported by Russian Science Foundation (RSF) grant 14-31-00024. The authors acknowledges the staff of I.M.Sechenov First Moscow State Medical University and especially Philip Kopylov for giving us patient-specific data.

REFERENCES

[1] Lucas O. Mller and Eleuterio F. Toro, A global multiscale mathematical model for the human circulation with emphasis on the venous system, *IJNMBE*, **30(7)**, 681–725, 2014.

[2] J. Alastruey, S. M. Moore, K. H. Parker, T. David, J. Peir, S. J. Sherwin, Reduced modelling of blood flow in the cerebral circulation: Coupling 1-D, 0-D and cerebral autoregulation models, *International Journal for Numerical Methods in Fluids*, **56(8)**, 1061–7, 2008.

[3] T.M. Gamilov, P.Y. Kopylov, R.A. Pryamonosov, S.S. Simakov, Virtual fractional flow reserve assessment in patient-specific coronary networks by 1D hemodynamic model, *RJNAMM*, **30(5)**, 269–276, 2015.

[4] S.S. Simakov, T.M. Gamilov TM, Y.N. Soe, Computational study of blood flow in lower extremities under intense physical load , *RJNAMM*, **28(5)**, 485–504, 2013.

[5] I. B. Wilkinson, J. R. Cockcroft, D. J. Webb. Pulse wave analysis and arterial stiffness *J. Cardiovasc. Pharmacol.*, **32, Suppl.3**, S33–7, 1998.

[6] W.F. Ganong, *Review of Medical Physiology*, Stamford, CT, Appleton and Lange, 1999.

[7] A.F. Frangi et al., Multiscale Vessel Enhancement Filtering. *Medical Image Computing and Computer-Assisted InterventationMICCAI98*, **1496**, 130–137, 1998.

[8] T.S. Yoo, M. J. Ackerman, W. E. Lorensen, W. Schroeder, V. Chalana, S. Aylward, D. Metaxas, R. Whitaker, Engineering and Algorithm Design for an Image Processing API: A Technical Report on ITK - The Insight Toolkit, In Proc. of *Medicine Meets Virtual Reality*, J. Westwood, ed., IOS Press Amsterdam 586-592, 2002.

[9] L. Grady, Fast, Quality, Segmentation of Large Volumes – Isoperimetric Distance Trees. *Computer Vision – ECCV 2006*, **3953**, 3711-3723, 2007.

[10] H.A. Gratama van Andel, Removal of Bone in CT Angiography by Multiscale Matched Mask Bone Elimination. *Medical Physics*, **34**, 3711-3723, 2007.

[11] A. Danilov, Yu. Ivanov, R. Pryamonosov, Yu. Vassilevski, Methods of Graph Network Reconstruction in Personalized Medicine. *International Journal for Numerical Methods in Biomedical Engineering*, 2015. doi: 10.1002/cnm.2754

k	l, cm	d, cm	c, cm/s	R, $\frac{kba \cdot s}{cm^3}$	k	l, cm	d, cm	c, cm/s	R, $\frac{kba \cdot s}{cm^3}$
1	3.05	2.99	600		44	2.29	0.34	700	
2	1.21	2.42	700		45	0.46	0.92	700	
3	14.9	0.74	700		46	2.72	0.29	700	50
4	15.34	0.4	700		47	8.40	0.72	700	
5	0.24	0.25	700		48	1.75	0.34	700	50
6	0.77	0.28	700		49	5.27	0.60	700	50
7	1.43	0.23	700		50	0.81	1.00	700	
8	0.56	0.17	700	25	51	7.11	0.25	700	50
9	1.64	0.16	700	25	52	0.42	1.10	700	
10	1.72	0.18	700		53	2.79	0.49	700	
11	2.76	0.76	700		54	3.02	0.96	700	
12	0.51	0.39	700		55	26.9	0.28	700	
13	1.30	0.37	700		56	2.15	0.83	700	
14	2.14	0.38	700		57	0.78	0.49	700	
15	4.55	0.35	700		58	0.55	0.31	700	25
16	0.27	0.29	700		59	1.04	0.24	700	25
17	8.82	0.18	700	100	60	0.41	0.7	700	
18	0.59	0.16	700	100	61	2.05	0.42	700	
19	6.98	0.24	700	100	62	2.25	0.19	700	25
20	5.48	0.27	700		63	4.48	0.23	700	25
21	4.37	0.19	700	100	64	0.17	0.69	700	
22	1.59	0.16	700	100	65	2.15	0.34	700	25
23	8.84	0.19	700	100	66	7.57	0.66	700	
24	1.36	0.19	700	100	67	1.62	0.29	700	25
25	4.66	1.25	700		68	6.58	0.59	700	25
26	9.56	0.75	910		69	3.36	1.07	700	
27	19.8	0.42	910		70	3.05	2.27	600	
28	0.22	0.21	700		71	7.94	2.39	600	4
29	0.29	0.15	700		72	3.04	0.18	700	10
30	0.24	0.26	700		73	1.27	0.19	700	
31	0.46	0.23	700		74	0.91	0.53	700	
32	1.25	0.20	700		75	2.30	0.47	700	
33	1.70	0.16	700	10	76	0.40	0.45	700	
34	2.11	0.19	700		77	1.38	0.34	700	
35	2.50	0.18	700		78	4.79	0.35	700	
36	0.63	0.18	700	10	79	3.48	0.22	700	37.5
37	3.12	0.23	700		80	7.54	0.23	700	37.5
38	3.58	0.24	700		81	7.65	0.21	700	37.5
39	2.55	0.19	700	25	82	11.4	0.18	700	37.5
40	4.34	0.18	700	25	83	7.06	0.23	700	37.5
41	2.77	0.27	700		84	1.59	0.25	700	37.5
42	22.9	0.39	700		85	0.8	0.22	700	
43	1.3	0.21	700	50	86	1.0	0.40	700	

Table 2: Parameters of the artery network shown in Fig. 2: k is the index of the vessel, l is the length, d is the diameter, c is the stiffness ((3)), R is the resistance (7). Veins are considered to have the same structure with c_k lowered by 20% and dubled d.